Inorg. Chem. **2007**, *46*, 5608–5615

Preparation of Au(I), Ag(I), and Pd(II) N-Heterocyclic Carbene Complexes Utilizing a Methylpyridyl-Substituted NHC Ligand. Formation of a Luminescent Coordination Polymer

Vincent J. Catalano* and Anthony O. Etogo

Department of Chemistry, University of Nevada, Reno, Nevada 89557

Received February 9, 2007

Reaction of the imidazolium N-heterocyclic carbene precursor containing a methyl-substituted pyridyl functionality [$HCH_3im(CH_3py)$]PF_6, **1**, with Ag_2O produces the homoleptic Ag(I) complex, [$Ag(CH_3im(CH_3py))_2$]PF_6, **2**. In a simple carbene transfer reaction the analogous Au(I) species, [$Au(CH_3im(CH_3py))_2$]PF_6, **3**, is formed by treatment of **2** with Au(tht)Cl in dichloromethane. Both **2** and **3** are structurally similar with nearly linearly coordinated NHC ligands. The methyl group appended to the pyridyl ring inhibits rotation of the pyridyl group at room temperature. Addition of $AgBF_4$ to a hot propionitrile solution of **3** followed by crystallization with diethyl ether yields the one-dimensional coordination polymer, $\{[AuAg(CH_3im(CH_3py))_2(NCCH_2CH_3)](BF_4)_2\}_n$, **4**, which contains Au–Ag separations of 2.9845(5) and 2.9641(5) Å with intermetallic angles of 167.642(14)° and 162.081(9)°. This material is intensely luminescent in the solid state and exhibits an emission band at 453 nm (λ_{ex} = 350 nm). Nearly colorless [$Pd(CH_3im(CH_3py))_2Cl$]PF_6, **5**, is produced upon treatment of **2** with $PdCl_2(NCC_6H_5)_2$. The Pd(II) center in **5** is coordinated to one NHC ligand in a chelate fashion, while the second NHC is bound solely through the carbon center. The X-ray crystal structures of **1**–**5** are reported.

Introduction

Recently, we reported the preparation and optical properties of several luminescent Au(I)−Ag(I) N-heterocyclic carbene (NHC) coordination polymers assembled using pyridyl-substituted N-methylimidazole backbones.[1] The first polymer, based on the symmetric py_2im ligand[2] (Chart 1), consists of helical chains of two-coordinate Au(I) centers alternately linked to three-coordinate Ag(I) centers spanned by two NHC−pyridyl linkages and a coordinated acetonitrile molecule.[3] One pyridyl group on each py_2im ligand appears unnecessary and remains uncoordinated in the polymeric structure. The metal−metal separations are short with Au(I)−Ag(I) linkages of 2.8359(4) and 2.9042(4) Å. This polymer is intensely luminescent in the solid state (λ_{max} = 515 nm) but dissociates into its monometallic precursors upon dissolution in donor solvents.

To explore the role of the uncoordinated pyridyl ring on the aforementioned dynamic behavior, the redundant pyridyl group was replaced with a simple methyl group (CH_3impy[4] in Chart 1). Four polymers, $\{[AuAg(CH_3impy)_2(L)](BF_4)_2\}_n$ and $\{[AuAg(CH_3impy)_2(NO_3)]NO_3\}_n$ where L is CH_3CN, C_6H_5CN, or $C_6H_5CH_2CN$ were produced. Each possesses similar two-coordinate, homoleptic Au(I) centers connected to trigonally coordinated Ag(I) centers containing two pyridyl groups and either a nitrile molecule or a coordinated nitrate anion. Changing the auxiliary ligands greatly influences the connections between the metal units, and in contrast to helical polymer observed with the py_2im ligand, a series of seemingly unrelated, distorted zigzag polymers are observed in the CH_3impy system. All of these polymers contain fairly short metal−metal separations ranging from 2.8 to 2.9 Å with the nitrate-containing polymer exhibiting both the shortest and longest Au(I)−Ag(I) separations of 2.8125(2)

Chart 1

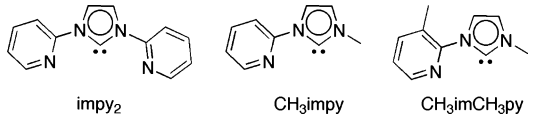

* To whom correspondence should be addressed. E-mail: vjc@unr.edu.

(1) Catalano, V. J.; Etogo, A. O. *J. Organomet. Chem.* **2005**, *690*, 6041.
(2) Chen, J. C. C.; Lin, I. J. B. *Organomentallics* **2000**, *19*, 5113.
(3) Catalano, V. J.; Malwitz, M. A.; Etogo, A. O. *Inorg. Chem.* **2004**, *43*, 5714.
(4) Grünedemann, S.; Kovacevic, A.; Albrecht, M.; Faller, J. W.; Crabtree, R. H. *J. Am. Chem. Soc.* **2002**, *124*, 10473.

10.1021/ic070260i CCC: $37.00
Published on Web 06/05/2007

Scheme 1

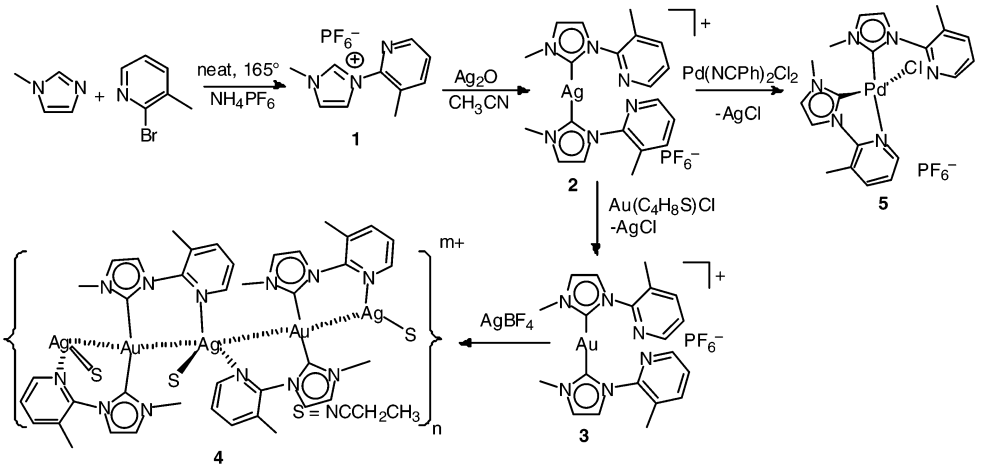

and 2.9482(2) Å. The benzonitrile containing polymer is the most regular with 2.833(1) and 2.835(1) Å Ag(I)−Au(I) separations. In the solid state, all of these polymers are photoluminescent with emission bands centered at 469, 474, 480, and 522 nm for $\{[AuAg(CH_3impy)_2(NO_3)]NO_3\}_n$ and $\{[AuAg(CH_3impy)_2(L)](BF_4)_2\}_n$, and (L = C_6H_5CN, CH_3CN, $C_6H_5CH_2CN$), respectively. The origin of the observed trend in emission behavior is not understood nor is it easy to assess given the variability in metal−core structures observed upon simple solvent ligation. Like the preceding $impy_2$-containing polymer, the CH_3impy polymers also dissociate into their monometallic components upon dissolution, demonstrating that the extra pyridyl ring is not responsible for the observed lability. Additionally, replacing the weak nitrile donor with the anionic nitrate ion also does not prevent dissociation in solution.

In an attempt to further explore the role of ligand architecture on polymer formation, we have investigated the role of placing a methyl substituent on the 3-position of the pyridyl ring, anticipating that the resulting steric encumbrance with the imidazole hydrogen would limit pyridyl rotation and, hence, retard dissociation. This work describes the preparation of a new pyridyl-substituted NHC ligand and its complexation to Ag(I) and Au(I). To test whether the added methyl group is sufficiently bulky enough to prevent a coplanar arrangement between the imidazole and pyridine portions of the CH_3imCH_3py ligand, the cis chelation of this ligand on Pd(II) species is explored. In the extreme case, an orthogonal orientation of these groups would prohibit chelation. Conversely, in the absence of hindrance, the imidazole−pyridyl moiety is an effective chelating ligand with Pd(II).[5−7]

Results

As shown in Scheme 1, the carbene precursor, $[HCH_3im(CH_3py)]PF_6$, **1**, was prepared in a manner similar to the preparation of CH_3impy first reported by Chen and Lin.[7] A mixture of 2-bromo-3-methylpyridine and 1-methylimidazole was heated neat at 165 °C for 14 h. The resulting bromide salt was metathesized to the hexafluorophosphate salt to produce **1** as an off-white powder in 35% yield. The carbene precursor **1** reacts with Ag_2O in CH_2Cl_2 in the presence of aqueous NaOH to form the homoleptic complex, $[Ag(CH_3im(CH_3py))_2]PF_6$, **2**. This material is then treated with Au(tht)Cl (tht is tetrahydrothiophene) to produce $[Au(CH_3im(CH_3py))_2]PF_6$, **3**, in a simple carbene transfer reaction. Analogously, treatment of **2** with $Pd(NCPh)_2Cl_2$ produces $[Pd(CH_3im(CH_3py))_2Cl]PF_6$ **5**, which contains a Pd(II) center with one chelating $CH_3im(CH_3py)$ ligand and one carbene bound NHC ligand. Addition of $AgBF_4$ to the gold monomer, **3**, in hot propionitrile produces the mixed-metal, Ag(I)−Au(I) coordination polymer, $\{[AuAg(CH_3im(CH_3py))_2(NCCH_2CH_3)](BF_4)_2\}_n$, **4**, upon crystallization. Conversely, under similar conditions no reaction is observed between $AgBF_4$ and $[Pd(CH_3im(CH_3py))_2Cl]PF_6$, indicating the chelated pyridine ring is inert to substitution. The gold and silver compounds are slightly sensitive to room light upon prolonged exposure, but solutions of **5** appear stable indefinitely.

In CD_3CN the ^1H NMR spectrum of the ligand precursor $[HCH_3im(CH_3py)]PF_6$ displays eight resonances including six in the aromatic region assigned to the imidazole and pyridine ring protons and the diagnostic singlet appearing at 8.82 ppm assigned to proton on C at the 1-position of the imidazolium ring. The remaining backbone protons on the imidazole ring resonate at 8.45 and 7.74 ppm, while the imidazole and pyridine ring methyl resonances are observed at 3.95 and 2.36 ppm, respectively. Coordination to Ag(I) to form $[Ag(CH_3im(CH_3py))_2]PF_6$, **2** eliminates the downfield resonance and shifts the imidazole backbone resonances to 7.38 and 7.33 ppm. The methyl resonance originally observed at 3.95 ppm moves upfield to 3.83 ppm, while the methyl resonance that was observed at 2.36 ppm is now split into two signals of equal intensity at 2.13 and 2.09 ppm indicative of two orientations for the pyridine methyl group on each ligand. Replacing the Ag(I) ion of **2** with Au(I) to form **3** results in only subtle changes in the imidazolium backbone resonances relative to those of **2** and are now observed at

(5) Danopoulos, A. A.; Tsoureas, N.; Green, J. C.; Hursthouse, M. B. *Chem. Commun.* **2003**, 756.
(6) Gründemann, S.; Albrecht, M.; Kovacevic, A.; Faller, J. W.; Crabtree, R. H. *J. Chem. Soc., Dalton Trans.* **2002**, *10*, 2163.
(7) Chen, J. C. C.; Lin, I. J. B. *Organometallics*, **2000**, 5113.

Table 1. X-ray Crystallographic Data for Complexes **1**−**5**

	1	**2**	**3**	**4**	**5**
formula	$C_{20}H_{24}F_{12}N_6P_2$	$C_{20}H_{22}AgF_6N_6P$	$C_{20}H_{22}AuF_6N_6P$	$C_{23}H_{27}AuAgB_2F_8N_7$	$C_{20}H_{22}ClF_6N_6PPd$
fw	689.36	599.28	688.37	879297	633.26
cryst syst	triclinic	monoclinic	monoclinic	monoclinic	monoclinic
space group	$P\bar{1}$	$P2_1/n$	$P2_1/n$	Cc	$P2_1/n$
a, Å	9.0762(3)	13.3884(6)	13.263(3)	12.9666(9)	12.4099(5)
b, Å	10.2474(4)	7.5058(3)	7.5648(15)	20.1452(14)	15.5311(6)
c, Å	15.1786(5)	23.8413(11)	23.783(5)	11.7021(8)	12.5353(5)
α, deg	86.9290(10)	90	90	90	90
β, deg	86.5840(10)	105.8810(10)	105.067(4)	110.0200(10)	104.9210(10)
γ, deg	64.7210(10)	90	90	90	90
V, Å^3	1273.65(8)	2304.38(17)	2304.3(8)	2872.1(3)	2334.58(16)
Z	2	4	4	4	4
temp, K	100(2)	100(2)	100(2)	100(2)	100(2)
R1	0.0495	0.0284	0.0478	0.0348	0.0203
wR2 ($I > 2\sigma(I)$)	0.1262	0.0728	0.1354	0.0764	0.0540

Table 2. Selected Bond Distances (Å) and Angles (deg) for **1**

C(1)−N(1)	1.318(3)	C(2)−C(3)	1.355(3)
C(1)−N(2)	1.337(3)	N(2)−C(5)	1.444(3)
N(1)−C(2)	1.377(3)	N(1)−C(4)	1.468(3)
N(2)−C(3)	1.387(3)	C(6)−C(10)	1.509(3)
N(1)−C(1)−N(2)	109.0(2)	N(1)−C(2)−C(3)	107.5(2)
C(1)−N(1)−C(2)	108.77(19)	N(2)−C(3)−C(2)	106.4(2)
C(1)−N(2)−C(3)	108.37(19)	C(1)−N(2)−C(5)−N(3)	54.9(3)

7.32 and 7.29 ppm. The methyl resonances remain nearly unchanged at 3.82, 2.13, and 2.10 ppm. Replacing Ag(I) with Pd(II) to form **5** completely transforms the ^{1}H NMR spectrum. The imidazole backbone protons in **5** now resonate downfield at 7.96 and 7.25 ppm, and the methyl region of the spectrum shows four singlets in a 1:1:1:1 ratio at 4.04, 3.40, 2.66, and 2.29 ppm consistent with two different coordination modes of the NHC ligand.

Additionally, the carbene region of the ^{13}C{^{1}H} NMR spectrum of **2** displays a sharp singlet at 181.80 ppm with no ^{13}C−^{107,109}Ag coupling. In **3** this resonance is observed at 184.84 ppm. The ^{1}H NMR spectrum for the polymer system is identical to that of **3**, indicating that this material dissociates completely into its monomers upon dissolution.

X-ray-quality crystals of **1**−**3** and **5** were obtained by slow diffusion of Et_2O into CH_3CN. Crystallographic data are presented in Table l. The ligand precursor, **1**, crystallizes in the triclinic space group $P\bar{1}$ with two cations and two hexafluorophosphate anions residing in the asymmetric unit. Selected bond distances are shown in Table 2, while an X-ray structural drawing depicting one-half of the asymmetric unit is displayed in Figure 1. The metrical parameters in both cations are typical of imidazole-based NHC precursors. The average $C_{carbene}$−N separation is 1.328(3) Å, and in both cations the imidazole and pyridyl rings are twisted with respect to each other with C(1)−N(2)−C(5)−N(3) and C(11)−N(5)−C(15)−N(6) torsion angles of 54.9(3)° and 56.0(3)°.

The colorless complex **2** crystallizes in the monoclinic space group $P2(1)/n$ with one cation and the hexafluorophosphate anion residing in the asymmetric unit. Selected bond distances are presented in Table 3. As shown in Figure 2, the two NHC ligands are nearly linearly coordinated to the Ag center with a C(1)−Ag(1)−C(11) angle of 171.69(6)° and Ag(1)−C(1) and Ag(1)−C(11) separations of 2.0945(15) and 2.0888(15) Å, respectively. The pyridyl rings

Table 3. Selected Bond Distances (Å) and Angles (deg) for **2** and **3**

	2 (M = Ag)	**3** (M = Au)
M(1)−C(1)	2.0888(15)	2.037(9)
M(1)−C(11)	2.0945(15)	2.026(9)
C(1)−N(1)	1.3464(19)	1.336(12)
C(1)−N(2)	1.3631(18)	1.392(11)
C(11)−N(4)	1.3545(18)	1.348(12)
C(11)−N(5)	1.3577(19)	1.370(12)
C(1)−M(1)−C(11)	171.69(6)	173.9(4)
C(1)−N(2)−C(5)−N(3)	41.5(2)	45.1(12)
C(11)−N(5)−C(15)−N(6)	100.35(17)	85.2(11)

Table 4. Selected Bond Distances (Å) and Angles (deg) for **4**

Au(1)−Ag(1)	2.9845(5)	C(1)−Au(1)−C(11)	174.4(2)
Au(1)−Ag(1A)	2.9641(5)	N(3)−Ag(1)−N(6)	147.38(17)
Au(1)−C(1)	1.995(6)	N(3)−Ag(1)−N(7)	107.51(18)
Au(1)−C(11)	2.007(6)	N(6)−Ag(1)−N(7)	103.89(19)
Ag(1)−N(3)	2.243(5)	N(1)−C(1)−N(2)	103.6(5)
Ag(1)−N(6)	2.267(5)	N(4)−C(11)−N(5)	105.1(5)
Ag(1)−N(7)	2.378(5)	Ag(1)−N(7)−C(21)	172.6(5)
N(7)−C(28)	1.143(8)	C(1)−N(2)−C(5)−N(3)	71.5(7)
Au(1)−Ag(1)−Ag(1A)	167.642(14)	C(11)−N(5)−C(15)−N(6)	52.9(6)
Ag(1)−Au(1)−Ag(1A)	162.081(9)		

are rotated such that their methyl groups reside on the same face of the cation. The torsion angles between the pyridyl and imidazole rings diverge from those in the precursor with C(1)−N(2)−C(5)−N(3) and C(11)−N(5)−C(15)−N(6) at 41.5(2)° and 83.9(2)°, respectively. The average $C_{carbene}$−N separation of 1.380(2) Å is only slightly longer than the corresponding value (1.328(3) Å) observed in **1**, indicating little backbonding from the metal to the NHC ligands.[8] There are no short metal−metal interactions, and the shortest Ag···Ag separation is long at 6.832 Å.

The analogous Au(I) monomer **3** is isostructural with **2** with nearly identical metrical and cell parameters (Tables 1 and 3). As displayed in Figure 3, coordination about the Au(I) center is almost linear with a C(1)−Au(1)−C(11) bond angle of 173.9(4)°. The two imidazole rings are nearly coplanar while the pyridyl groups are rotated about 45.15(2)° and 85.22(2)° relative to their respective imidazole rings. As expected, the Au(1)−C(1) and Au(1)−C(11) separations of 2.037(9) and 2.026(9) Å are slightly shorter than the corresponding metal−carbon distances in **2**. There are no short aurophilic contacts in **3**, and the shortest Au···Au contact is long at 6.888 Å.

(8) Nemcsok, D.; Wichmann, K.; Frenking, G. *Organometallics* **2004**, *23*, 3640.

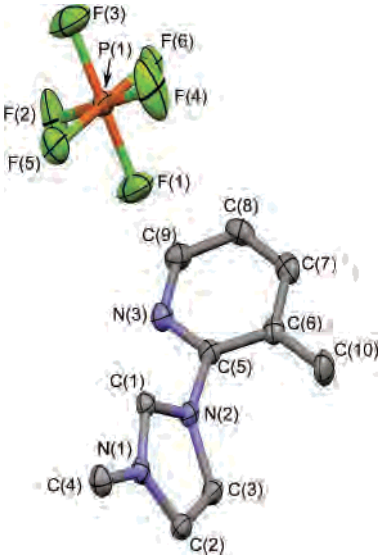

Figure 1. Thermal ellipsoid plot (50%) of one-half of the asymmetric unit of **1**. Hydrogen atoms removed for clarity.

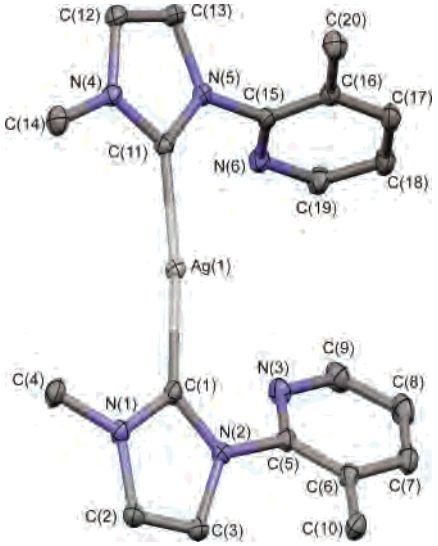

Figure 2. X-ray structural drawing of cationic portion of **2** drawn with 50% thermal ellipsoids and hydrogen atoms omitted.

X-ray quality crystals of **4** were grown by slow diffusion of Et_2O into a propionitrile solution containing $[Au(CH_3im)(CH_3py))_2]PF_6$ and excess $AgBF_4$. Polymer **4** crystallizes in the monoclinic, non-centrosymmetric space group *Cc* with the dimetallic repeating unit and two tetrafluoroborate anions comprising the asymmetric unit. Selected bond distances and angles are presented in Table 4, while a structural drawing of the cationic portion of the asymmetric unit and the extended polymer chain are displayed in Figure 4. The polymetallic core consist of repeating Au(1)−Ag(1) units with separations of 2.9845(5) and 2.9641(5) Å and alternating intermetallic Au(1A)−Ag(1)−Au(1) and Ag(1A)−Au(1)−Ag(1) angles of 167.64(1)° and 162.081(9)°, respectively. The Au(I) center is two-coordinate and nearly linearly coordinated to two NHC ligands with a C(1)−Au(1)−C(11) angle of 174.4(2)° and Au(I)−C(1) and Au(I)−C(11) bond distances of 1.995(6) and 2.007(6) Å, respectively. The Ag(I) center is bound to two pyridyl rings from alternating Au-

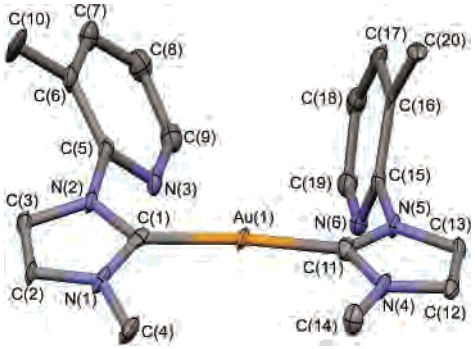

Figure 3. Thermal ellipsoid plot (50%) of cationic portion of **3**.

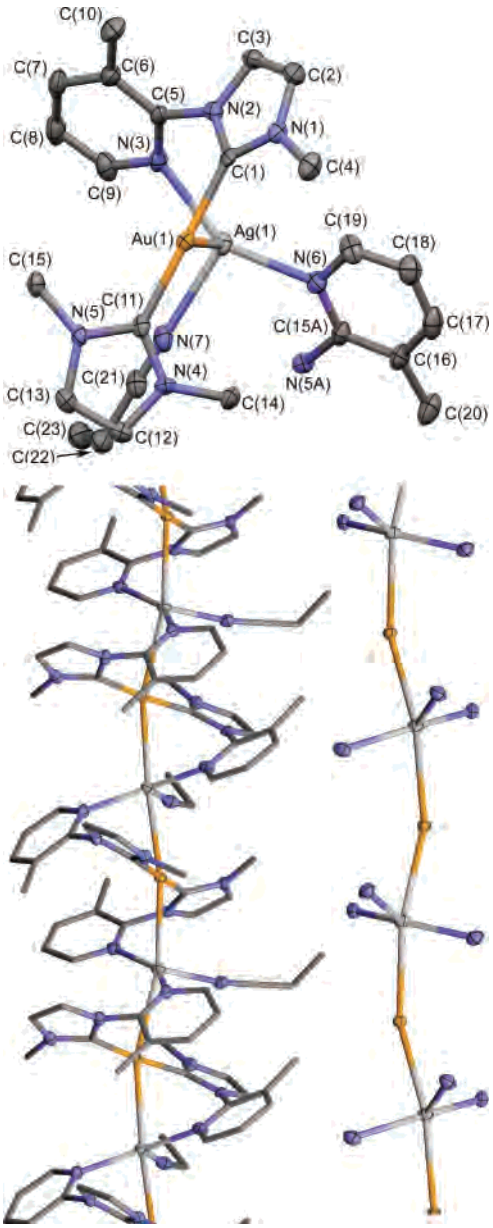

Figure 4. X-ray structural drawing of cationic portion of asymmetric unit (top) of **4** and extended polymeric chain (bottom, left) and polymer core (bottom, right). Thermal ellipsoids are drawn at 50%.

(I) centers and a single propionitrile molecule. This metal center maintains a trigonal planar environment with N(3)−Ag(1)−N(6), N(3)−Ag(1)−N(7), and N(6)−Ag(1)−N(7) angles of 147.38(17)°, 107.51(18)°, and 103.89(19)°, re-

Table 5. Selected Bond Distances (Å) and Angles (°) for **5**

Pd(1)−C(1)	1.9625(10)	C(1)−N(1)	1.3399(14)
Pd(1)−C(11)	1.9707(10)	C(1)−N(2)	1.3758(13)
Pd(1)−Cl(1)	2.3385(3)	C(11)−N(4)	1.3463(13)
Pd(1)−N(3)	2.0801(9)	C(11)−N(5)	1.3541(13)
C(1)−Pd(1)−N(3)	78.72(4)	C(11)−Pd(1)−N(3)	174.16(4)
C(1)−Pd(1)−C(11)	95.70(4)	C(1)−Pd(1)−Cl(1)	172.78(3)
N(3)−Pd(1)−Cl(1)	96.09(3)	C(1)−N(2)−C(5)−N(3)	2.83(13)
Cl(1)−Pd(1)−C(11)	89.31(3)	C(11)−N(5)−C(15)−N(6)	82.91(13)

spectively. The sum of these angles is 358.8°, close to the required 360° angle required for planarity. The propionitrile−silver separation at 2.378(5) Å (Ag(1)−N(7)) is slightly longer than the pyridyl−silver separations of 2.243(5) and 2.267(5) Å for Ag(1)−N(3) and Ag(1)−N(6), respectively. Within the propionitrile molecule the C(21)−N(7) separation at 1.143(8) Å is typical of a triple bond. The nitrile moiety is nearly linearly coordinated to the Ag(I) center with a C(21)−N(7)−Ag(1) angle of 172.6(5)°. The pyridyl and imidazole rings are significantly distorted from coplanarity with C(1)−N(2)−C(5)−N(3) and C(11)−N(5)−C(15)−N(6) torsion angles of 71.5(7)° and 52.9(6)°, respectively. The larger twisting of the N(3)-containing ligand prevents a "direct-on" approach of the pyridyl ring lone pair to the Ag center. Consequently, the angle defined by the pyridyl ring centroid, N(3) and Ag(1) at 162.26° is less than the ideal 180°. The corresponding angle in the less-twisted N(6)-containing ligand registers at 176.94°. Interestingly, this twisting appears to have little effect on the metal−pyridyl separation, and in fact, the Ag(1)−N(3) separation is 0.026 Å shorter than the Ag(1)−N(6) separation.

Nearly colorless **5** crystallizes in the monoclinic space group *P*2(1)/*n* with only the cation and a hexafluorophosphate anion residing in the asymmetric unit. Selected bond distances and angles are presented in Table 5, while a structural drawing of the cationic portion is shown in Figure 5. As shown, one NHC ligand coordinates in bidentate fashion while the other is attached solely through the carbene portion of the ligand trans to the pyridyl group of the bidentate NHC. The remaining coordination site is occupied by a chloride ligand. The Pd(II) center adopts a pseudo-square-planar geometry. The sum of the angles around Pd(II) is 359.8° with two obtuse C(11)−Pd(1)−C(1) and N(3)−Pd(1)−Cl(1) angles of 95.70(4)° and 96.09(3)°, respectively, and two acute C(11)−Pd(1)−Cl(1) and N(3)−Pd(1)−C(1) angles of 89.31(3)° and 78.72(4)°, respectively. The trans angles, C(1)−Pd(1)−Cl(1) and N(3)−Pd(1)−C(11), are almost linear at 172.78(3)° and 174.16(10)°. The NHC ligands are closely bound to the Pd-center with Pd(1)−C(1) and Pd(1)−C(11) separations of 1.9625(10) and 1.9701(10) Å, respectively. The remaining pyridyl and chloride ligand−metal separations are longer with Pd(1)−N(3) and Pd(1)−Cl(1) bond distances of 2.0801(5) and 2.3385(3) Å, respectively. The rigid chelating nature of the bidentate NHC ligand is evident and forces the pyridyl and imidazole ring to be nearly coplanar with a C(1)−N(2)−C(5)−N(3) torsion angle of only 2.83(13)° while in the monodentate NHC ligand, these two groups are nearly orthogonal to each other as reflected by the C(11)−N(5)−C(15)−C(16) torsion angle of

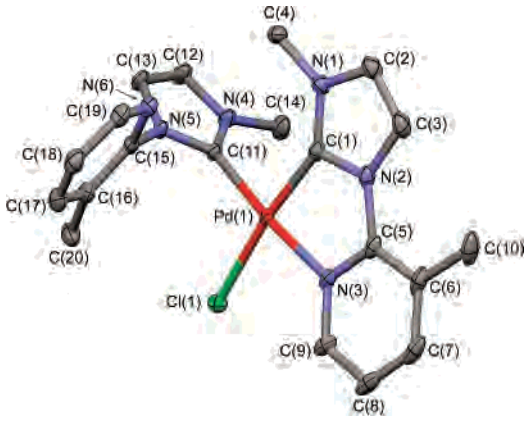

Figure 5. Thermal ellipsoid plot (50%) of cationic portion of **5** with hydrogen atoms omitted for clarity.

82.91(12)°. Additionally, the angle between the two imidazole portions of the ligands is large at 78.45°.

The electronic absorption spectra of these complexes are unremarkable. All of the complexes contain $\pi-\pi^*$ transitions well into the ultraviolet portion of the electromagnetic spectrum. Complexes **2** and **3** have nearly identical spectra with bands between 260 and 280 nm analogous to the ligand precursor **1**. Because **4** dissociates in solution, its electronic absorption spectrum mimics that of its gold precursor, **3**. Likewise, the Pd-containing complex contains similar bands at 210 and 264 nm.

Polymer **4** is visibly luminescent in the solid state at room temperature when excited with a hand-held UV lamp (λ_{ex} = 336 nm). Both solution and solid-state samples of the carbene precursor are also photoluminescent with a band appearing at 446 nm. Excitation of a solid sample at 380 nm of the monometallic Au containing species **3** produces a broad emission band at 472 nm. At room temperature the solid-state emission spectrum of polymer **4** shows an intense band at 453 nm (λ_{ex} = 350 nm).

Discussion

This chemistry provides additional support for the generality of one-dimensional Au(I)−Ag(I) achiral and chiral coordination polymer formation utilizing the structurally rigid pyridyl−imidazolium linkage. The lack of flexibility in this linkage likely constrains the Ag(I) center to a very strained pseudo-trigonal-planar environment which is easily disrupted in solution. Incorporation of a methyl group in the 3-position of the pyridyl group does indeed hinder rotation of the pyridyl group, but unexpectedly, does not significantly impact the pyridyl binding, as evidenced by the relatively short pyridyl−silver separations in **4**. Like the previously prepared pyridyl−imidazole polymers, the structure of **4** appears to be very sensitive to ligation. Simple modifications such as exchanging the coordinated solvent dramatically alter the metal−metal separations and angles making direct comparisons difficult. Likewise, polymer **4** is best described as a zigzag polymer with comparatively long Au(I)−Ag(I) separations of 2.9641(5) and 2.9845(5) Å and intermetallic angles of 167.642(14)° and 162.081(9)°. These metal separations are the longest observed thus far in this class of

polymers. For comparison, the analogous separations in the closely related $\{[AuAg(CH_3impy)_2(NCCH_3)](BF_4)_2\}_n$ polymer range from 2.8633(6) to 2.9239(6) Å, with larger deviations in the intermetallic angles which range from 135.20(2)° to 175.37(3)°. Although it is tempting to ascribe this structural difference to the presence of the added methyl group on the pyridyl ring, similar deviations are observed between $\{[AuAg(CH_3impy)_2(NCCH_3)](BF_4)_2\}_n$ and $\{[AuAg(CH_3impy)_2(NCC_6H_5)](BF_4)_2\}_n$, which differ only in the ligated solvent.

Polymer **4** is the sixth in the series of achiral and chiral coordination polymers obtained by utilizing pyridyl−imidazolium ligands reported so far. Silver-containing coordination polymers,[9,10] as well as species with mixed-metal interactions[11] are not uncommon. The heterometallic interactions have often been shorter than homometallic interactions, and recent reports have attributed this to the attractive dipolar interactions between dissimilar metals.[12−14] Additionally, the Au(I)−Ag(I) separations observed in **4** compare well with those observed by Fernández, Laguna, and co-workers[15] in the decanuclear, carboxylate-bridged polymer that contains short, mixed-metal separations of 2.8226(4) and 2.8993(4) Å. A shorter Au(I)−Ag(I) separation of 2.8245(6) Å is found in the mesityl, tetrahydrothiophene-bridging dinuclear polymer, $[\{(PPh_3)Au(\mu\text{-mes})(\mu\text{-tht})Ag]^{2+}\}_n$[16] while longer Au(I)−Ag(I) distances (2.9010(6)−3.0134(6) Å) are found in the carboxylate-bridged, square pyramidal Au_4Ag cluster, $[Au(3,5\text{-}C_6Cl_2F_3)_2Ag_4(CF_3CO_2)_5]^{2-}$.[17]

The crystal structure of the polymer **4** is non-centrosymmetric, yet the bulk material is achiral. Like $\{[AuAg(impy_2)_2(NCCH_3)](BF_4)_2\}_n$ and $\{[AuAg(CH_3impy)_2(NCC_6H_5)](BF_4)_2\}_n$, individual crystals of **4** are non-centrosymmetric, but the bulk material is racemic. Spontaneous resolution of racemic Ag-containing polymers from achiral components, although rare, have been reported elsewhere.[18−21]

Interestingly, the room-temperature solid-state emission spectrum of polymer **4** displays a band at 453 nm. This is significantly blue-shifted relative to the emission maxima of the previously reported nitrile containing polymers, $\{[AuAg(CH_3impy)_2(L)](BF_4)_2\}_n$, (L is C_6H_5CN, CH_3CN, $C_6H_5CH_2CN$) which under similar conditions exhibits bands at 474, 480, and 522 nm, respectively. Because the metal−metal separation and angles are different in each polymer, it is not possible to ascribe this blue-shift to the electronic or steric factors from the added methyl group or to the shortened Au(I)−Ag(I) separations observed in **4**. The origin of this differential luminescence likely resides in a combination of factors such as metal chain geometry and ancillary ligand electronic and steric properties, but without a homologous series of polymers, these factors cannot be differentiated. We are working toward this goal.

In the Pd(II) complex **5**, the NHC ligand binds both as a monodentate and a bidentate ligand, further demonstrating that the steric hindrance of the pyridyl methyl group can be mitigated by expanding the imidazole−pyridyl linkage angle in the chelated $CH_3im(CH_3py)$ ligand (C(3)−N(2)−C(5) = 131.51(9)°) compared to that in the monodentate ligand (C(13)−N(5)−C(15) = 122.79(9)°). Further, in the chelated ligand the imidazole ring and the pyridyl ring are nearly coplanar with an interplanar angle of only 6.25°, suggesting that there the added methyl group has almost zero influence on chelate ring formation. In fact, this angle is very similar to the 5.95° angle observed by Chen and Lin[7] in the analogous unmethylated $[Pd(impy_2)Br]^+$ species. Clearly a larger group is needed to prevent chelation; however, increasing the steric bulk too much would likely inhibit polymer formation for the related Au complex.

The Pd−Cl and Pd−N bonds of 2.3385(3) and 2.0801(5) Å are longer than those Pd−Cl (2.2859−2.305 Å) and Pd−N (2.010−2.040 Å) bonds found in trans dichloro[22−24] and dipyridine[25−27] compounds. These larger values are consistent with the relatively large trans-influence of the carbene.[28] However, the Pd(1)−N(3) linkage proved to be very strong, and attempts to open this ring using chloride or cyanide were unsuccessful.

Last, because complexes **2** and **3** isostructural, they provide a unique opportunity to explore the relativistic contraction of Au compared to Ag. Using the M−C separations to calculate the covalent radii, the Au(I) ion appears smaller than the Ag(I) ion by 0.051−0.068 Å. This effect is slightly smaller than the ∼0.1 Å contraction measured in the bis(trimesitylphosphine) gold and silver complexes reported by

(9) Khlobystov, A. N.; Blake, A. J.; Champness, N. R.; Lemenovskii, D. A.; Majouga, A. G.; Zyk, N. V.; Schröder, M. *Coord. Chem. Rev.* **2001**, *222*, 155.

(10) Chiu, P. L.; Chen, C. Y.; Zeng, J. Y.; Lu, C. Y.; Lee, H. M. *J. Organomet. Chem.* **2005**, *690*, 1682.

(11) Xu, C.; Anderson, G. K.; Brammer, L.; Braddock-Wilking, J.; Rath, N. P. *Organometallics* **1996**, *15*, 3972−3979.

(12) Catalano, V. J.; Malwitz, M. A. *J. Am. Chem. Soc.* **2004**, *126*, 6560.

(13) Rawashdeh-Omary, M. A.; Omary, M. A.; Fackler, J. P., Jr. *Inorg. Chim. Acta* **2002**, *334*, 376.

(14) Fernández, E. J.; Laguna, A.; López-de-Luzuriaga, J. M.; Monge. M.; Pyykkö, P.; Runeberg, N. *Eur. J. Inorg. Chem.* **2002**, 750.

(15) Fernández, E. J.; Laguna, A.; López-de-Luzuriaga, J. M.; Montiel, M.; Olmos, M. E.; Pérez, J.; Puelles, R. C. *Organometallics*, **2006**, 4307.

(16) Conte, M.; Jiménez, J.; Jones, P. G.; Laguna, A.; Laguna, M. *J. Chem. Soc. Dalton Trans.* **1994**, 2525.

(17) Fernández, E. J.; Laguna, A.; López-de-Luzuriaga, J. M.; Monge, M. Montiel, M.; Olmos, M. E.; Pérez, J.; Puelles, R. C.; Sáenz, J. C. *Dalton Trans.* **2005**, 1162.

(18) Janiak, C. *Dalton Trans.* **2003**, 2781.

(19) Janiak, C.; Scharmann, T. G.; Albrecht, P.; Marlow, F.; Macdonald, R. *J. Am. Chem. Soc.* **1996**, *118*, 6307.

(20) Bu, X.-H.; Chen, W.; Du, M.; Biradha, K.; Wang, W.-Z.; Zhang, R.-H. *Inorg. Chem.* **2002**, *41*, 437.

(21) Abrahams, B. F. Jackson, P. A.; Robson, R. *Angew. Chem., Int. Ed. Engl.* **1998**, *37*, 2656.

(22) Qin, Z.; Jenkins, H. A.; Coles, S. J.; Muir, K. W.; Puddephatt, R. J. *Can. J. Chem.* **1999**, *77*, 155.

(23) Meij, A. M. M.; Muller, A.; Roodt, A. *Acta Crystallogr.* **2003**, *E59*, m44.

(24) Onoda, A.; Kawakita, K.; Okamura, T.; Yamamoto, H.; Ueyama, N. *Acta Crystallogr.* **2003**, *E59*, m291.

(25) Goddard, R.; Green, M.; Hughes, R. P.; Woodward, P. *J. Chem. Soc., Dalton Trans.* **1976**, 1890.

(26) Viossat, B.; Dung, N.-H.; Robert, F. *Acta Crystallogr., Sect. C* **1993**, *49*, 84.

(27) Vicente, J.; Abad, J.-A.; Fernández-de-Bobadilla, R.; Jones, P. G.; Romairez-de-Arellano, M. C. *Organometallics* **1996**, *15*, 24.

(28) Scott, N. M.; Nolan, S. P. *Eur. J. Inorg. Chem.* **2005**, 1815.

Schmidbaur and co-workers[29] but is closer to the 0.07 Å contraction observed by Laguna and co-workers[30] in the mixed-valent, phosphide-bridged Au(I)Au(III) complex, PPN-[{Au(C_6F_5)$_3$(μ-PPh$_2$)}$_2$Au]. Shorter Au(I)−C than Ag(I)−C separations are freqently observed in NHC chemistry. Our previous work on [M(impy$_2$)]$^+$ (M = Ag or Au) complexes[3] shows a fairly large average difference in separation of 0.093 Å, while a smaller difference of 0.073 Å is observed in the related [M(CH$_3$impy)$_2$]$^+$ system.[1] Likewise, the Ag(I)−C separations in the picolyl-substituted NHC complexes, [M(im(CH$_2$py)$_2$)$_2$]$^+$, are 0.061 Å longer than their Au(I)−C counterparts.[3] These observations are consistent with the data from an extensive review by Garrison and Youngs[31] who examined numerous Ag−NHC complexes and reported an average Ag(I)−C_{NHC} bond length of 2.087(5) Å with a fairly small range of 2.06(1)−2.117(5) Å. A similar analysis of the 28 [Au(NHC)$_2$]$^+$ complexes found in the Cambridge Crystallographic Data Center yields an average Au(I)−C_{NHC} separation of 2.020 Å and a range of 1.986−2.066 Å. Globally, an average 0.067 Å decrease in Au−C separation relative to Ag−C for NHC complexes is calculated.

Conclusions

While the added methyl group in the 3-position on the pyridyl group influences the dynamic behavior of the CH$_3$-im(CH$_3$py) ligand, it is not sterically encumbered enough to lock this group into position, and the resulting polymer, **4**, readily dissociates in solution. Likewise, this ligand forms a rigid chelate with Pd(II) and is resistant to opening, further supporting the notion that the presence of the appended methyl group does not greatly influence pyridyl binding. More interesting are the longer metal−metal separations observed in **4** and the blue-shifted emission in the solid state. These data further support the idea that subtle modifications to the polymer composition lead to dramatic changes in structure and optical properties.

Experimental Section

Solvents were used as received without purification or drying. The preparations of Au(tht)Cl[32] and PdCl$_2$(NCPh)$_2$[33] were described elsewhere. ^{1}H NMR spectra were recorded on a Varian Unity+ NMR spectrometer operating at 500 MHz and 25 °C. Chemical shifts are reported relative to TMS but were measured on the basis of the internal solvent peak. UV−vis spectra were obtained using a Hewlett-Packard 8453 diode array spectrometer (1 cm path-length cells). Emission data were recorded using a Spex Fluoromax steady-state fluorimeter.

Preparation of 1. A mixture of 2-bromo-3-methylpyridine (1.544 g, 8.9 mmol) and 1-methylimidazole (0.737 g, 8.9 mmol) was heated neat at 165 °C for 14 h. After cooling, the resulting dark red oil was diluted with 30 mL of water, followed by addition of an aqueous solution containing 1.95 g (12.0 mmol) of NH_4PF_6. The precipitated solid was isolated by filtration and washed with two 30 mL portions of anhydrous Et$_2$O to afford 1.01 g (13.4 mmol) of **1** as an off-white powder (35%). ^{1}H NMR (499.8 MHz, CD$_3$CN, 25 °C) δ 8.82 (s, 1H), 8.45 (d, 4.5 Hz, 1H), 7.94 (d, 7.0 Hz, 1H), 7.74 (m, 2.0 Hz 1H), 7.53 (m, 2.0 Hz, 1H), 3.95 (s, 3H), 2.63 (s, 3H). ^{13}C{^{1}H} NMR (100.5 MHz, CD$_3$CN, 25 °C) δ 147.57, 142.31, 136.59, 128.43, 126.39, 124.09, 122.68, 36.68, 16.97.

Preparation of 2. A 100 mL round-bottom flask was charged with 0.138 g (0.43 mmol) of [HCH$_3$im(CH$_3$py)]PF$_6$, 25 mL of CH$_2$-Cl$_2$, 0.020 g (0.088 mmol) of Ag$_2$O, and 10 mg of Bu$_4$NPF$_6$. The mixture was protected from light and stirred for 1.5 h at room temperature. NaOH (1 N, 3 mL) was then added, and stirring was continued for a further 15 min. The mixture was filtered through celite. The bright yellow filtrate was reduced to minimum volume under vacuum, and the product was precipitated with Et$_2$O affording 0.160 g (0.27 mmol) of **2** as a white powder (79%). ^{1}H NMR (499.8 MHz, CD$_3$CN, 25 °C) δ 8.32 (m, 4.5 Hz, 2H), 7.83 (m, 7.5 Hz, 2H), 7.46 (m, 1.0 Hz, 2H), 7.38 (d, 2.0 Hz, 2H), 7.33 (d, 2.0 Hz, 2H), 3.82 (s, 6H), 2.13 (s, 3H), 2.09 (s, 3H). ^{13}C{^{1}H} NMR (125.7 MHz, CD$_3$CN, 25 °C) δ 181.98, 151.67, 148.39, 142.73, 131.59, 126.66, 124.64, 123.37, 39.38, 17.84. UV (CH$_3$CN) λ_{max}, nm (ϵ): 212 (34 720), 276 (29 000), 315 (2100).

Preparation of 3. A 50 mL round-bottom flask was charged with 0.110 g (0.18 mmol) of **2** in 20 mL of CH$_3$CN. To this was added 0.059 g (0.18 mmol) of Au(tht)Cl dissolved in 10 mL of CH$_3$CN. The mixture was protected from light and stirred for 15 min, after which the solution was filtered through celite to remove the precipitated AgCl. The clear filtrate was reduced to minimum volume under vacuum, and the product was precipitated using Et$_2$O affording 0.099 g (0.14 mmol) of **3** as a white powder (80%). ^{1}H NMR (499.8 MHz, CD$_3$CN, 25 °C) δ 8.32 (d, 8.0 Hz, 2H), 7.77 (d, 12.5 Hz, 2H), 7.46 (m, 8.0 Hz, 2H), 7.32 (d, 3.5 Hz, 2H), 7.29 (d, 3.5 Hz, 2H), 3.82 (s, 6H), 2.13 (s, 3H). 2.10 (s, 3H) ^{13}C{^{1}H}NMR (125.7 MHz, CD$_3$CN, 25 °C) δ 184.84, 150.05, 147.12, 129.78, 125.77, 123.40, 125.87, 38.31, 17.31. (CH$_3$CN) λ_{max}, nm (ϵ): 219 (20 700), 265 (19 000).

Preparation of 4. A 100 mL round-bottom flask was charged with 0.071 g (0.10 mmol) of **3** and 0.060 g (0.31 mmol) of AgBF$_4$ in 30 mL of CH$_3$CH$_2$CN. The colorless mixture was protected from light and stirred at room temperature for 1.5 h. The mixture was filtered through bulk celite, reduced to minimum volume under vacuum, and the product was precipitated with Et$_2$O affording 0.075 g (0.04 mmol) of **4** as a white powder (43.8%).

Preparation of 5. A 100 mL round-bottom flask was charged with 0.129 g (0.22 mmol) of **2** in 30 mL of CH$_3$CN. To this was added 0.081 g (0.22 mmol) of Pd(C$_6$H$_5$CN)$_2$Cl$_2$. The mixture was protected from light and stirred for 45 min, after which the solution was filtered through celite to remove the precipitated AgCl. The orange-yellow filtrate was reduced to minimum volume under vacuum, and the product was precipitated using Et$_2$O affording 0.088 g (0.14 mmol) of **5** as a light yellow powder (86%). Anal. Calcd (%) for C$_{20}$H$_{22}$ClF$_6$N$_6$PPd: C, 37.93; H, 3.50; N, 13.27. Found: C, 37.63; H, 3.19; N, 13.09. ^{1}H NMR (499.8 MHz, CD$_3$-CN, 25 °C) δ 8.88 (d, 4.8 Hz, 1H), 8.18 (d, 4.2 Hz, 1H) 7.99 (d, 7.5 Hz, 1H), 7.96 (d, 2.1 Hz, 2H), 7.82 (d, 8.1 Hz, 1H), 7.50 (s, 5H), 7.40 (m, 3.9 Hz, 1H), 7.25 (d, 2.1 Hz, 2H), 4.04 (s, 3H), 3.40 (s, 3H), 2.66 (s, 3H), 2.29 (s, 3H). ^{13}C{^{1}H} NMR (125.7 MHz, CD$_3$CN, 25 °C) δ 146.95, 146.72, 146.66, 141.10, 131.35, 125.87, 124.71, 123.93, 123.35, 119.51, 38.30, 37.62, 19.95, 17.02. (CH$_3$-CN) λ_{max}, nm (ϵ): 210 (22 000), 264 (16 000).

X-ray Crystallography. X-ray-quality crystals were grown by slow vapor diffusion of diethyl ether into an acetonitrile solution of the complex. Suitable crystals were coated in a hydrocarbon oil

(29) Bayler, A.; Schier, A.; Bowmaker, G. A.; Schmidbaur, H. *J. Am. Chem. Soc.* **1996**, *118*, 7006.
(30) Blanco, M. C.; Fernández, E. J.; Jones, P. G.; Laguna, A.; López-de-Luzuriaga, J. M.; Olmos, M. E. *Angew. Chem., Int. Ed.* **1998**, *37*, 3042.
(31) Garrison, J. C.; Youngs, W. J. *Chem. Rev.*, **2005**, *105*, 3978.
(32) Usón, R.; Laguna, A.; Laguna, M. *Inorg. Synth.* **1989**, *26*, 85.
(33) Anderson, G. K.; Lin, M. *Inorg. Synth.* **1990**, *28*, 60.

and mounted on a glass fiber. X-ray crystallographic data were collected at low temperature (100 K) using a Bruker SMART Apex CCD diffractometer with Mo Kα radiation and a detector-to-crystal distance of 4.94 cm. Data were collected in a hemisphere using four sets of frames with 0.3° scans in ω and an exposure time of 10 s per frame. The 2θ range extended from 3.0° to 64°. Data were corrected for Lorentz and polarization effects using the SAINT program and corrected for absorption using SADABS. Unit cells were refined using up to 9999 reflections harvested from the data collection. The structures were solved by direct methods and refined using the SHELXTL 6.10 software package.[34]

Acknowledgment. This work and the X-ray diffractometer purchase were supported by the National Science Foundation (CHE-0549902 and CHE-0226402).

Supporting Information Available: Crystallographic data in CIF format for **1**−**5**. This material is available free of charge via the Internet at http://pubs.acs.org.

IC070260I

(34) Sheldrick, G. M. *SHELXTL: Structure Determination Software Suite, Version 6.10*; Bruker AXS: Madison WI, 2001.